Stephen Schlecht ORCID iD: 0000-0002-6857-927X

Morphology of mouse ACL-complex changes following exercise during pubertal growth

Stephen H. Schlecht, Ph.D[1,2*], Colin T. Martin, B.Sc[3], Danielle N. Ochocki[3], Bonnie T. Nolan[1], Edward M. Wojtys, MD[1], James A. Ashton-Miller, Ph.D[2]
[1]Department of Orthopaedic Surgery, University of Michigan, Ann Arbor, 48109
[2]Department of Mechanical Engineering, University of Michigan, Ann Arbor, 48109
[3]Department of Chemistry, University of Michigan, Ann Arbor, 48109
*Corresponding author: Department of Orthopaedic Surgery, 2228 Biomedical Science Research Building, 109 Zina Pitcher Place, Ann Arbor, MI, 48109. Tel: 734-647-1528; Email: sschlech@med.umich.edu
Running Title: Exercise effect on growing ACL-complex
Author contributions: Study Design – SHS, BTN, EMW, JAAM. Data Collection – SHS, CTM, DNO, BTN. Data Interpretation – SHS, CTM, DNO, EMW, JAAM. Manuscript Preparation - SHS, CTM, DNO, EMW, JAAM. Manuscript Approval - SHS, CTM, DNO, BTN, EMW, JAAM.

Abstract

Postnatal development and the physiological loading response of the anterior cruciate ligament (ACL) complex (ACL proper, entheses, and bony morphology) is not well understood. We tested whether the ACL-complex of two inbred mouse strains that collectively encompass the musculoskeletal variation observed in humans, would demonstrate significant morphological differences following voluntary cage-wheel running during puberty compared to normal cage activity controls. Female A/J and C57BL/6J (B6) 6-week-old mice were provided unrestricted access to a standard cage-wheel for 4 weeks. A/J-exercise mice showed a 6.3% narrower ACL ($p = 0.64$), and a 20.1% more stenotic femoral notch ($p < 0.01$) while B6-exercise mice showed a 12.3%

wider ACL (p = 0.10), compared to their respective controls. Additionally, A/J-exercise mice showed a 5.3% less steep posterior medial tibial slope (p = 0.07) and an 8.8% less steep posterior lateral tibial slope (p = 0.07), while B6-exercise mice showed a 9.8% more steep posterior medial tibial slope (p < 0.01) than their respective controls. A/J-exercise mice also showed more reinforcement of the ACL tibial enthesis with a 20.4% larger area (p < 0.01) of calcified fibrocartilage (CF) distributed at a 29.2% greater depth (p = 0.02) within the tibial enthesis, compared to their controls. These outcomes suggest exercise during puberty significantly influences ACL-complex morphology and that inherent morphological differences between these mice, as observed in their less active genetically similar control groups, resulted in a divergent phenotypic outcome between mouse strains.

Introduction

The impact of physiological loading on the postnatal development of the anterior cruciate ligament (ACL) complex (i.e., the ACL proper, entheses, and bony morphology) is not well understood. An increase in the strength and/or stiffness of the ACL in response to exercise throughout growth has been reported in animal models[1,2]. Viidik[1] showed that high frequency exercise in skeletally immature rabbits increased ACL strength, particularly at the tibial entheses, while Cabaud et al.[2] demonstrated that endurance exercise increased ACL interstitial strength and stiffness in growing rats. However, neither of these studies reported on the influence exercise during musculoskeletal growth has on the morphological traits encompassing the ACL-complex. This includes ACL size, the calcified fibrocartilaginous matrix within the femoral and tibial entheses, as well as the distal femoral and proximal tibial epiphyseal morphology comprising the knee joint. To date, Grzelak and colleagues[3] provide the only known report attributing activity to a 3.5-fold larger ACL cross-sectional area among high performance weightlifters that began training as adolescents compared to age-matched

controls. However, this magnetic resonance study included only nine athletes and was dependent on self-reporting.

Clinically, associations between several morphological traits of the knee and ACL injury risk have been widely reported in both sexes across various ages and sport activities. These morphological risk factors, which *in vitro* studies have found to increase the likelihood of ACL impingement[4], anterior tibial translation[5,6] and/or increased ACL peak strains[7,8], include ACL cross-sectional area[7,9], femoral intercondylar notch width/shape[10,11], and posterior tibial plateau slope[12,13]. How the morphology of these anatomical traits is biomechanically influenced throughout growth via differentially applied physiological loads is of considerable clinical importance yet remains unclear. Interestingly, Tuca et al.[14] recently reported their findings from an MRI study conducted on boys and girls ranging from 3 – 14-years old that suggested the significant growth in ACL volume and femoral intercondylar notch volume plateaued by 10 years of age in both sexes. Their finding supports the prevailing dogma of the field that these morphological traits are largely non-modifiable after the pre-pubescence phase[15]. However, the findings of Tuca and colleagues[14] research is inconsistent with other musculoskeletal studies conducted on high activity individuals. Bone[16-18], muscle[19-21], and tendinous size[22,23] are significantly different morphologically in the dominantly loaded musculoskeletal element of individuals compared to their non-dominant contralateral and in comparison to individuals that had a lower activity level throughout growth (both pre- and post-puberty)[3,16,24-28].

In light of the uncertainty surrounding how the knee joint and associated ACL traits are affected following increased mechanical loading during postnatal growth, we tested two hypotheses using a mouse model (A/J and C57BL/6J) with a phenotypically similar knee structure as humans[29]. Our previous pilot work found that A/J mice exhibit a slender knee joint morphology with narrow femoral and tibial condyles, a stenotic intercondylar

femoral notch, a narrow ACL, and a narrow tibial plateau. They also have moderately sloped medial and lateral posterior tibial plateaus and broad yet shallow ACL entheses (i.e., uncalcified and calcified fibrocartilaginous zones demarcated by a tidemark that functionally anchor the ligament into bone). On the other hand, C57BL/6J (B6) mice have a robust knee joint morphology with wide femoral and tibial condyles, a parabolic intercondylar femoral notch, a wide ACL, and a broad tibial plateau. Additionally, they have severely sloped medial and lateral posterior tibial plateaus and narrow yet deep ACL entheses. Moreover, A/J and C57BL/6J (B6) mice have differing knee joint mechanics with A/J mice previously shown having a 68% ($p < 0.001$) greater joint laxity and a lower ($p = 0.003$) toe region stiffness compared to B6 mice at musculoskeletal maturity[30]. Using this model, which collectively encompasses the variation in knee joint morphology observed across male and female humans[7,13,31,32], we first tested the hypothesis that pubescent (6 – 10 weeks of age) exercised mice of both inbred strains would show significant phenotypic differences in their ACL-complex morphology, particularly in regards to ACL cross-sectional area and intercondylar notch width, compared to their normal cage activity controls. Additionally, since the knee joint phenotype naturally differs between A/J and B6 mice we also tested the hypothesis that the resulting outcome 4-weeks of increased physiological loading would have on traits comprising the ACL-complex would be different between these two mouse strains. This was tested by defining the post-exercise differences in ACL size, calcified fibrocartilage distribution (reflective of ACL bone anchorage footprint), and bone morphology between mouse strains.

Previously, we reported a significantly larger bone mass in the femoral ($p = 0.01$) and humeral ($p = 0.02$) diaphyses and distal femora ($p = 0.02$) following voluntary exercise between 8-week old A/J females compared to their controls. This morphological change was not observed in their exercised B6 counterparts[33]. Based on these outcomes, we also

hypothesized that the gracile knee of A/J mice would show a greater expansion of the intercondylar notch, ACL, and calcified fibrocartilage within the femoral and tibial ACL entheses at 10-weeks of age following exercise when compared to exercised B6 mice.

Characterizing the morphology of ACL-complex traits following an increase in pubescent activity will shed light on how an increase in physiological loading during a critical musculoskeletal growth phase may or may not influence the resulting adult knee morphology. Moreover, it will help us to better understand indirectly the influence physiological loading upon the ACL-complex may have on the inherent baseline metabolic[34,35] and musculoskeletal[36,37] differences that exist between A/J and B6 mice. The overarching clinical importance of this study is to determine whether it is feasible for ACL-complex morphological traits commonly associated with ACL injury risk to be biomechanically susceptible to an increase in physical activity during the pubescent growth phase.

Methods

Choice of age at entry and duration of the study were chosen to coincide with the hormonal fluctuations and rapid skeletal growth occurring during murine puberty. Six-weeks-of-age in mice is the average at which puberty begins[38,39], and 10-weeks-of-age is the average at which mice reach sexual maturity – a biological indicator of adulthood[40]. Twenty-four female A/J and 24 female B6 inbred mice were purchased from the Jackson Laboratory (Bar Harbor, ME, USA) at five-weeks-of-age and allowed one week to acclimate before the start of the study. For each strain, mice were block randomized into a control (n = 12) or exercise group (n = 12). Mice were distributed into each group using body weight to ensure that all groups were similar in size at the start of the study ($p > 0.50$). Mice in both the control and exercise groups were individually housed for the duration of the study. All mice were provided water and fed a standard rodent diet (D12450B; Research Diets, New Brunswick, NJ, USA) *ad libitum*. Mice were kept on a

12-hour light/dark cycle and provided a nestlet for cage enrichment. A/J and B6 mice assigned to the exercise group (n = 12/strain) had free access (24 hours/day) to a stainless-steel cage wheel (115 mm outer diameter; Mini-Mitter Co., Inc., Murrysville, PA, USA) for 4 weeks. Wheel revolutions were monitored daily, and the distance run (km) was calculated as the number of revolutions *times* the outer diameter of the wheel *times* π. Control mice were allowed normal cage activity during the study. Body weight (BW) and food weight (FW) were recorded one time per week throughout the course of the experiment. Mice were euthanized at 10-weeks-of-age and the left and right legs (n = 12/group/strain) were harvested, cleaned of all soft tissue leaving only the knee joint intact, and stored in 1x phosphate-buffered saline (PBS) solution at -40° C. The Institutional Animal Care and Use Committee (IACUC) at the University of Michigan approved all handling and treatment of mice for this study. Table 1 defines trait abbreviations that are frequently used throughout the article.

ACL morphology

The knee joint of the left and right legs from both control and exercise mice were dissected using a Leica S6E stereo microscope equipped with a Leica EC3 digital color camera (Leica Microsystems, Inc., Buffalo Grove, IL, USA). The infrapatellar fat pad, collateral ligaments, menisci, and posterior cruciate ligament were carefully removed, leaving only the ACL intact. Due to the small and relatively fragile nature of the specimens, the posterolateral and anteromedial bundles of the ACL could not be separated. Following dissection, the knee was imaged in the coronal and sagittal planes using the stereo microscope for quantification of the maximum posterior length (ACL.Post.Le) and posterior and medial widths (ACL.Post.Wi and ACL.Med.Wi) of the ACL. Measurements were taken using ImageJ (NIH) to calculate ellipsoidal cross-sectional area (ACL Ell.CSA).

Knee joint morphology

After imaging the ACL for areal quantification, the legs were fixed for 72 hours in 10% neutral buffered formalin. Upon fixation, each ACL was transected midsubstance for three-dimensional imaging of the femora and tibiae of each mouse. All bones were imaged while submerged in 1x PBS at an 8-μm voxel size using nano-computed tomography (nanotom-s, GE Sensing and Inspection Technologies, GmbH, Wunstorf, Germany). Imaging parameters were set to 90 kV, 375 μA, 1000 ms. 3 averages, and 1 skip, with a 0.3 mm aluminum filter. Grey values were converted to Hounsfield units using a calibration phantom containing air, water, and a hydroxyapatite mimicker (1.69mg/cc; Gammex, Middleton, WI, USA) as described previously[37].

Image analysis was conducted using Microview Advanced Bone Analysis (v. 2.2, GE Healthcare) and VGStudio (Volume Graphics, Inc., Charlotte, NC, USA). Maximum femoral (Fem.Le) and tibial (Tib.Le) lengths were measured from the image stacks. For femoral analysis, bones were anatomically reoriented, and the slices used for analysis were standardized based on morphological landmarks. Several measurements of the intercondylar femoral notch were made in accordance with Fitch et al.[41] and Comerford et al.[42]. These measures included the anterior (Ant.Not.Wi), central (Cen.Not.Wi), and posterior (Post.Not.Wi) notch widths, intercondylar notch height (Not.Ht), and bicondylar width (Fem.Bicon.Wi) (Fig. 1A). Variables derived from these measures included notch width indices (i.e., ANWI: Ant.Not.Wi/Fem.Bicon.Wi; CNWI: Cen.Not.Wi/Fem.Bicon.Wi; and PNWI: Post.Not.Wi/Fem.Bicon.Wi) and an estimate of the femoral notch shape (NSI: Cen.Not.Wi/Not.Ht).

Similar to the femora, tibiae were reoriented, and slices used for analysis were defined based on morphological landmarks. Methods used for obtaining measurements from the tibial plateau were in accordance with Reif and Probst[43]. Briefly, the longitudinal axis of the tibia was defined as the middle of the tibial intercondylar

eminences through the center of the talar articular surface. A line perpendicular to this axis was then defined along the medial and lateral plateau surfaces. The angle between the posterior medial and lateral plateau surfaces and the perpendicular line was quantified, providing the degree of posterior medial (PMTS) and posterior lateral (PLTS) tibial slope for each tibia (Fig. 1B). The bicondylar width of the tibial plateau (Tib.Bicon.Wi) was also measured.

Entheseal histomorphometry

Following three-dimensional imaging of the femora and tibiae, all bones were decalcified in 10% ethylenediamine tertraacetic acid (EDTA) for ten days, dehydrated through graded alcohols, and embedded in paraffin. For the femoral and tibial blocks, sagittal 7-µm serial sections were taken across the entire ACL enthesis. Paraffin sections were then stained with 1% toluidine blue (Sigma-Aldrich, St. Louis, MO, USA), a monochromatic stain that highlights the 4 matrix zones of the ACL enthesis (i.e., ligament proper, uncalcified fibrocartilage (UF), calcified fibrocartilage (CF), and bone). Stained histologic sections were imaged at 10x magnification under polarized light using a Nikon Eclipse (*Ni*; Nikon, Melville, NY, USA) microscope affixed with a digital color camera (*DS-Ri2*; Nikon, Melville, NY, USA). Using NIS Elements software (Nikon, Melville, NY, USA), the length of the tidemark (TM.Le), calcified fibrocartilage area (CF.Ar), and the depth of the calcified fibrocartilage (CF.De) were measured as they are reliably quantifiable and directly associated with the anchorage of the ACL into bone. TM.Le was defined as the total expanse of the basophilic line running from the anterior to the posterior margins of the ACL insertion[32] which provides a measure of ACL insertion width. CF.Ar was defined as the differentially stained region between the TM and cortical bone. CF.De was defined as the perpendicular distance from the TM to the edge where the CF meets cortical bone. To account for the heterogeneity in CF.De across the

enthesis, measurements were taken at 30 μm intervals across the enthesis resulting in ~5–8 zones depending on the expanse of the ACL insertion[44] (Fig. 2A-B).

Data Analyses

All data were analyzed using Minitab v.18 (State College, PA, USA) and Prism v.7 (GraphPad Software, La Jolla, CA, USA). A Shapiro-Wilk test was conducted to determine if the data were normally distributed. All data was normalized via linear regression to the respective body weight at sacrifice of each mouse. Body weight was chosen to adjust the data since a percentage of the total body mass provides an external force during axial loading of the knee joint[45,46] , and influences ground-reaction force[47,48]. Adjusted trait values were entered into a two-way analysis of variance (ANOVA) to test for strain and treatment (exercise, control) main effects, and strain by treatment interaction with a significance of $p < 0.10$. Tukey multiple comparisons test between exercised and control mice within and between strains were assessed to determine the significance of least square mean differences in the presence of important interactions. Following this, linear regression analysis was used to identify significant associations between body weight adjusted phenotypic traits and distance-run.

To test for intraobserver reliability when selecting landmarks for measuring ACL.Le, ACL.Wi, PMTS, and PLTS, each of these variables were measured three separate times from all mice included in the study, one month apart. Intraclass coefficient values obtained from this test demonstrated good to excellent reliability for ACL.Le (0.885), ACL.Post.Wi (0.936), ACL.Med.Wi (0.921), and PLTS (0.871). PMTS demonstrated moderate reliability with an ICC value of 0.631.

Results

Table 2 is comprised of mean and standard deviation data for each key trait quantified, after adjusting for body weight. Table 3 includes linear regression data

showing how each trait is associated with the total distance run of each mouse in the study, after adjusting for body weight.

Effect of distance run on body weight

At the onset of the running study, mice comprising the control and exercise groups for both strains were sorted so there was no significant difference in mean body weight both within strain groups (A/J: $p = 0.82$; B6: $p = 0.66$) and across strain groups (Controls: $p = 0.57$; Exercise: $p = 0.51$). After 4-weeks of running, A/J-exercise mice showed a non-significant ($p = 0.19$) 3.49% lower body weight compared to controls, while B6-exercise mice significantly gained 13.2% more weight (20.9 ± 1.0 g; $p < 0.01$) than their controls (18.4 ± 1.2 g). Despite A/J-exercise mice ending with less weight and B6-exercise mice ending with more weight than their respective controls, both exercise groups consumed significantly more food throughout the study (A/J-exercise: 23%, $p < 0.01$; B6-exercise: 20%, $p < 0.01$) compared to their controls.

Over the course of 4-weeks, A/J-exercise mice had a daily average of distance run that was 10% more (9.28 ± 2.1 km) than B6-exercise mice (8.42 ± 1.7 km), however this was not a significant difference ($p = 0.27$) (Fig. 3) since at the onset of the study A/J was slower to adjust to the wheel. Both A/J-exercise and B6-exercise mice ran significantly more in the 4th week of the study than they did during the 1st week of the study ($p < 0.01$ and $p = 0.03$, respectively).

Exercise effect on differences in ACL size

Without exercise, A/J-control mice at 10-weeks-of-age had an ACL that was 4.0% smaller than that of their B6 counterparts ($p = 0.87$). This non-significant difference was primarily driven by B6-control mice having a greater ACL.Le ($p < 0.01$) and ACL.Post.Wi ($p = 0.01$), compared to A/J-control mice. The difference in ACL Ell.CSA between strains was greater in the mice that ran with A/J-exercise mice having an ACL that was 26.7% smaller ($p < 0.01$) than that of B6-exercise mice. This differential effect

between strains is illustrated by the significant strain by treatment interaction (F = 7.61, p = 0.01). The dichotomy in ACL size is attributed to B6-exercise mice having a 13.5% significantly larger ACL Ell.CSA than B6-control mice (p = 0.05), and A/J-exercise mice showing a non-significant (p = 0.58) 6.8% smaller ACL Ell.CSA compared to controls. Interestingly, the more A/J mice ran the smaller ACL Ell.CSA was at 10-weeks-of-age (R^2 = 0.46, p = 0.03), whereas the more B6 mice ran the larger their ACL was at 10-weeks-of-age (R^2 = 0.41, p = 0.02) (Fig. 4).

Exercise effect on knee joint morphology

At 10-weeks-of-age A/J-control mice had a non-significant 2.4% narrower Fem.Bicon.Wi (p = 0.25) yet a significantly narrower femoral notch (ANWI: -29.8%, p < 0.01; CNWI: -21.5%, p < 0.01; PNWI: -15.8%, p < 0.01) compared to B6-control mice. However, there was no significant difference between the two control strains in NSI (p = 0.33). In mice that ran during the same four weeks of growth these morphological differences were greater with A/J-exercise mice showing a significantly narrower Fem.Bicon.Wi (-7.1%, p < 0.01) and narrower femoral notch width indices (ANWI: -34.6%, p < 0.01; CNWI: -33.1%, p < 0.01; PNWI: -26.1%, p < 0.01) compared to B6-exercise mice. Additionally, A/J-exercise mice showed a 23.4% more stenotic femoral notch (NSI: p < 0.01) compared to their B6 counterparts. This differential effect between strains is illustrated by the significant strain by treatment interaction for Fem.Bicon.Wi (F = 5.76, p = 0.02), CNWI (F = 2.82, p = 0.10) and PNWI (F = 6.36, p = 0.01), but not ANWI (F = 0.04, p = 0.84). The difference in distal femoral morphology between strains that ran is attributed to A/J-exercise mice having a narrower Fem.Bicon.Wi (-3.6, p = 0.03), femoral notch (ANWI: -9.4%, p = 0.46; CNWI: -9.5%, p = 0.04; PNWI: -6.4%, p = 0.04), and NSI (-19.1%, p < 0.01) compared to their controls. There was no significant difference in any of the distal femoral morphology measures between B6-exercise mice and their controls. There also was no significant association between the amount A/J and

B6 mice ran over the course of 4 weeks and their distal femoral morphology at 10-weeks-of-age.

Similar to the distal femoral morphology results, A/J-control mice at 10-weeks-of-age had a 5.0% narrower Tib.Bicon.Wi ($p < 0.01$) compared to B6-control mice. AJ-control mice also had less steep posterior tibial plateau slopes (PMTS: -3.2%, $p = 0.47$; PLTS: -33.5%, $p < 0.01$) compared to their B6 counterparts. In mice that ran, A/J-exercise mice showed a slight difference in Tib.Bicon.Wi (1.2%, $p = 0.19$), and even less steep posterior tibial slopes (PMTS: -19.2%, $p < 0.01$; PLTS: -40.3%, $p < 0.01$) compared to B6-exercise mice. This differential effect between strains is illustrated by the significant strain by treatment interaction for Tib.Bicon.Wi ($F = 22.51$, $p < 0.01$) and PMTS ($F = 24.13$, $p < 0.01$), but not PLTS ($F = 0.47$, $p = 0.496$). The difference in proximal tibial morphology is attributed to A/J-exercise mice having a 4.6% less steep PMTS ($p = 0.15$) and 8.2% less steep PLTS ($p = 0.11$) than their controls, while B6-exercise mice showed a 3.9% narrower Tib.Bicon.Wi ($p < 0.01$) a 10.2% steeper PMTS ($p < 0.01$) with a similar PLTS ($p = 0.59$) compared to their controls. There was no significant association between the amount A/J and B6 mice ran and their resulting proximal tibial morphology.

Exercise effect on femoral and tibial ACL entheseal morphology

Compared to B6-control mice at 10-weeks-of-age, A/J-control mice had a wider ACL insertion site, as inferred from the femoral and tibial tidemark (TM) measures of the ACL entheses (8.7%, $p = 0.40$ and 36.9%, $p < 0.01$; respectively). On the femoral side, A/J and B6-control mice had a similar CF.Ar ($p = 0.81$). However, the calcified fibrocartilage was heterogeneously distributed at an average 22.3% shallower depth in A/J-controls compared to B6-controls (Zones 2 – 4, $p = 0.05 – 0.002$). At the tibial ACL enthesis the wider TM among A/J-controls resulted in a 33.1% greater CF.Ar ($p < 0.01$) that, similar to the femoral side, was distributed at an average 22.8% shallower depth compared to B6-control mice (Zones 3 – 5, $p = 0.07 – 0.0001$). Within strains, exercise had no significant

effect on the femoral Fem.TM, CF.Ar, and CF.De present within the enthesis compared to their respective controls (Fig. 5A-B). However, there was a significant strain by treatment interaction for Fem.CF.Ar ($F = 5.69$, $p = 0.02$). Moreover, B6 showed a significant association between the amount they ran and their femoral ACL entheseal morphology, but only in the expanse of their Fem.TM ($R^2 = 0.59$, $p = 0.02$).

The results differed within the tibial enthesis. A/J-exercise mice showed an 18.2% narrower Tib.TM ($p < 0.01$) with 23.0% less CF.Ar ($p < 0.01$) and 24.4% greater average CF.De ($p = 0.08$) compared to their respective controls (Fig. 5C-D). In contrast, the CF.Ar and CF.De of the tibial ACL enthesis of B6-exercise mice was not significantly different than their controls. However, they did exhibit a deeper penetration of the calcified fibrocartilaginous matrix in the central portion of the enthesis (Zones 2 - 3, $p = 0.02 – 0.009$). The strain by treatment interaction was significant for Tib.TM ($F = 13.95$, $p < 0.01$) and CF.Ar ($F = 4.99$. $p = 0.03$), but not for average CF.De ($F = 0.22$, $p = 0.64$). There was no significant association between the amount A/J and B6 mice ran and their tibial ACL entheseal morphology.

Discussion

Our data support the first hypothesis that more physiological activity during pubertal growth showed greater morphological differences among traits comprising the ACL-complex in exercised inbred mice compared to their controls, particularly in ACL size and intercondylar femoral notch width. The results also support the second hypothesis that A/J and B6 mice would show a differing ACL-complex phenotype following increased physiological loading during growth. A/J-exercise mice showed a significantly narrower femoral bicondylar width and intercondylar notch size and shape compared to controls. They also had less steep posterior medial and lateral tibial plateaus, with greater anchorage of the ACL within the anteromedial portion of the tibial enthesis via deeper penetration of the calcified fibrocartilaginous matrix into bone. In contrast, B6-exercise

mice demonstrated little difference in knee morphology compared to their controls, with only a narrower tibial bicondylar width and a steeper posterior medial tibial plateau. However, B6-exercise mice did show a significantly more hypertrophic ACL compared to controls that was bolstered by deeper penetration of the calcified fibrocartilage into bone within the central portion of the tibial enthesis.

These outcomes did not support our last hypothesis that the ACL-complex of A/J exercise mice would be more robust overall than the gracile knee of A/J-control mice. Instead A/J-exercise mice demonstrated a narrower femoral bicondylar width resulting in a more stenotic intercondylar notch compared to controls. This narrower notch space among A/J-exercised mice may explain why they failed to demonstrate a significantly more hypertrophic ACL than their controls, since notch size may covary with ACL size to mitigate the likelihood of ACL impingement. Not only did A/J-exercise mice show a narrower distal femoral morphology than their controls but they also showed significantly less steep posterior medial and lateral tibial plateaus. Therefore, although A/J-exercised mice did not show a larger ACL Ell.CSA, a less steep posterior tibial slope in A/J-control mice may allow the knee joint of mice that ran to withstand greater physiological loading about the knee and perhaps protect the ACL from increased peak strains by reducing anterior tibial translation[49,50] compared to the less active controls. Moreover, the broader femoral ACL insertion and significantly deeper penetration of calcified fibrocartilage within the anteromedial portion of the tibial enthesis in A/J mice that ran may allow the ACL to dissipate applied strains more effectively, while better resisting anterior tibial load during knee extension [51,52], compared to their less active controls.

The difference in the ACL-complex between B6-control and exercise mice was also unexpected since previously we reported that B6 female mice that ran for 4 weeks during growth showed significantly narrower femoral and humeral diaphyses compared to controls[33]. Instead, B6-exercise mice showed no difference in the femoral side of the

knee joint compared to their controls. The only bony differences observed in B6-exercise mice was a 3.9% narrower tibial bicondylar width and a 10.2% steeper medial posterior tibial plateau. Clinically speaking, a very steep medial posterior tibial slope may be viewed as detrimental, however in the case of B6-exercise mice, the steeper medial plateau is more equivalent to that of the lateral plateau slope on (PMTS: 28.7° ± 0.1.3°, PLTS: 31.4° ±.2.0°), potentially allowing for greater joint stability by reducing the tendency for internal tibial rotation and thus greater ACL peak strains compared to less active controls. A minimization of ACL strain may have also be greater among B6 mice that ran since they show a 13.5% larger ACL and deeper penetration of calcified fibrocartilage within the central portion of the tibial enthesis compared to their less active controls.

It is widely reported that certain anatomical features of the knee joint are associated with increased ACL injury-risk in amateur and professional athletes[49,53]. Of particular concern is the fact that adolescent females are 1.6 times more likely to suffer an ACL-injury per athletic exposure compared to adolescent males[54]. The morphological traits attributed to this disparity are a narrow intercondylar femoral notch, a narrow ACL, and a steep posterior tibial plateau[7,49]. These traits are widely considered to be non-modifiable[13,15,55]. Findings from this murine study raise the possibility that these morphological risk factors may in fact be modifiable to some degree during growth, as both A/J and B6 mice exposed to greater physiological loading during puberty showed significant differences within their ACL-complex compared to their genetically similar and age-matched less active controls. However, the outcomes of this research also raise the specter that if morphological traits associated with increased ACL-injury risk are significantly influenced by exercise in children, training regimes would most likely need to be tailored to the individual, since the impact of greater physiological loading is likely dependent on an individual's unique set of traits, as evidenced by the differential

differences shown by A/J (gracile knee) and B6 (robust knee) mice that ran throughout puberty.

This is the first study to report that, with exercise during growth, genetically similar inbred mice can show morphological differences in the knee joint that are not present in normal cage activity controls. A strength of this study is the use of voluntary cage-wheel running as the activity perturbation. This mode of activity is physiologically relevant and allows for the detection of subtle effects in a manner that best mimics daily load experience by active teens during growth. Many studies incorporate forced treadmill running to mechanically perturb the musculoskeletal system and is done during working hours when the researcher is present. Voluntary cage-wheel running is cognizant of mouse nocturnal activity patterns and thus their circadian rhythms while minimizing physiological stressors (e.g., shock grid, high pressure air) that have been linked to elevated corticosterone levels, increased pro-inflammatory cytokines and anxiety[56]. Most importantly, voluntary cage-wheel running is more consistent with the endurance exercise capacity of mice, which is on average short running bursts of 150 revolutions at speeds that conform to those achieved during treadmill running[57]. Allowing nocturnal mice to voluntarily exercise resulted in both inbred strains running approximately 9 kilometers a night throughout the duration of the study. This is far greater than the average one mile per hour rate for 30 minutes/day other studies treadmill-exercise animals for to generate a phenotypic response[1,2,58]. Moreover, our mice ran approximately 250 kilometers by the completion of the study, compared to less than 100 kilometers in other studies, and were presumably less stressed while doing so, minimizing physiological and behavioral confounding factors.

However, there are several limitations within this study that caution against the over-interpretation of the results. First, this study did not focus on the cellular bone remodeling activity occurring within the knee joint of mice between the ages of 6 and 10 weeks.

Others have shown[59] that this physiological activity may vary between inbred mouse strains of the same age. For example, it may be that B6 mice demonstrated little bony differences with exercise because their skeletal growth was closer to plateauing than that of A/J mice. However, the purpose of our study was to investigate to what extent, if any, exercise had on the ACL-complex in growing mice with phenotypic differences that model the variation among traits comprising the knee joint that are present across humans. Second, the analysis of traits comprising the ACL-complex was performed at the end of the study. Thus, there were no baseline measures of these traits prior to the initiation of the study. This did not allow us to compare developmental changes of specific traits to distance run by each mouse. Since A/J-exercise mice showed a narrower ACL with running, and B6-exercise mice showed a wider ACL with running, it would be important to longitudinally track how these traits develop and are influenced by the underling genetics over time. The differential phenotype of the ACL may be attributed to previously reported metabolic differences that exist between the two mouse strains[60]. However, for almost every skeletally related trait there was no significant difference between the traits of mice comprising the exercise group in either strain and the number of revolutions they performed each day. This would suggest that the variation in distance run among mice was within the same activity threshold range for both strains[61]. Third, we did not mechanically test the tensile strength and stiffness of the ACL, and therefore are unable to determine whether the ACL showed a functional benefit to exercise as Viidik[1] and Cabaud et al.[2] observed. Moreover, we do not know whether the greater ACL Ell.CSA shown by B6-exercise mice translates to a greater mechanical benefit. Last, the resulting differential phenotypes shown in the exercise cohorts were only shown in female mice. It is unknown if males, which voluntarily run less on a daily basis[57] would show similar differences following exercise.

In conclusion, this study contributes to the discussion as to whether certain biological risk factors known to correlate with ACL injury are modifiable during growth. Our data confirmed our hypothesis that mice that run voluntarily during pubertal growth show a different knee morphology compared to those with normal cage activity. Moreover, we confirmed our hypothesis that the differences between A/J and B6 female control mice knee morphology would continue to differ in significantly new ways following 4-weeks of exercise during growth. Neither outcome has been previously reported. Collectively our findings suggest it may be possible to modify certain morphological traits comprising the ACL-complex during growth; however, the intervention chosen to adaptively direct a desired change is likely to be individual-specific.

Acknowledgements

This research was supported by a grant from the NIH National Institute of Arthritis and Musculoskeletal and Skin Diseases (SHS: AR070903). This research was also supported by the Michigan Integrative Musculoskeletal Health Core Center (NIH/NIAMS: AR065424). We would like to thank Dr. Melanie L. Beaulieu and Rebecca Falzon for comments and suggestions on earlier drafts of this manuscript.

Figures

Figure 1. Bone morphology measurements. A) Schematic of distal femoral epiphyseal anthropometric measurements. A = Ant.Not.Wi; B = Cen.Not.Wi; C = Post.Not.Wi; D = Tt. Con.Wi; and E = Not.Ht. B) Schematic of proximal tibial epiphyseal anthropometric measurements. Solid line represents the longitudinal axis of the tibia with the dotted lines representing the perpendicular and posterior tibial slope. NanoCT images at an 8 μm voxel size.

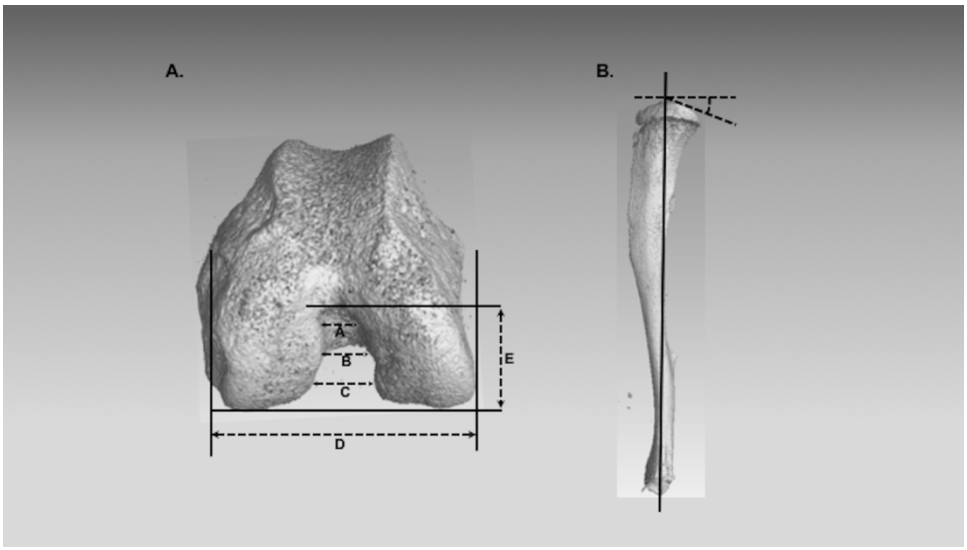

Figure 2. Calcified fibrocartilage measurements for A) femoral ACL enthesis and B) tibial ACL enthesis. Dotted black line indicates the tidemark. The red line indicates the boundary between the calcified fibrocartilage and bone. The solid black lines indicate the measurement of calcified fibrocartilage depth at 30 μm intervals along the tidemark. L = ligament and B = bone. Toluidine blue stain at 10x magnification.

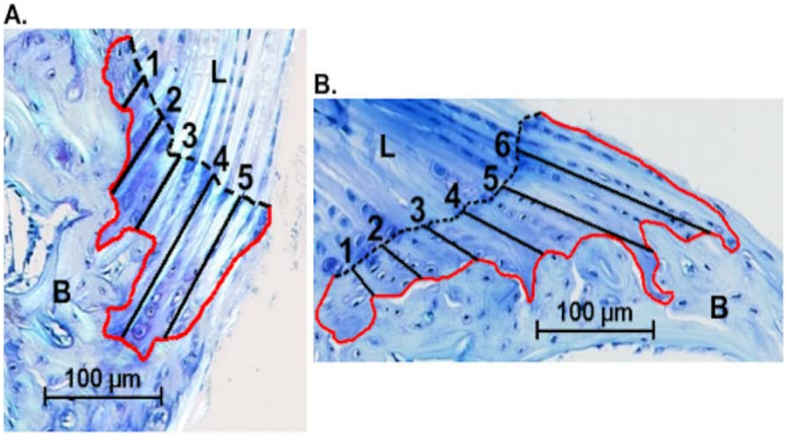

Figure 3. Average and standard deviations of daily distance run by voluntary cage wheel running mice of both inbred strains throughout the 4-week study.

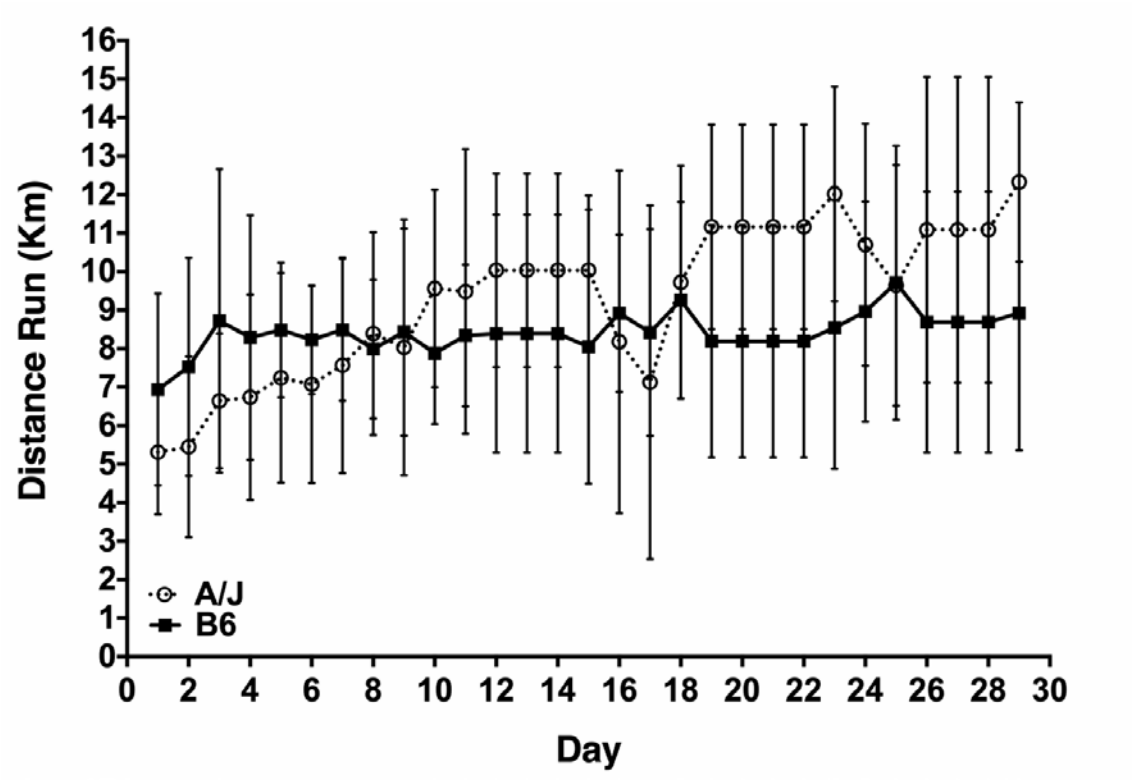

Figure 4. Linear regression showing the relationship between ACL Ell.CSA and daily distance run for both inbred strains after adjusting for body weight.

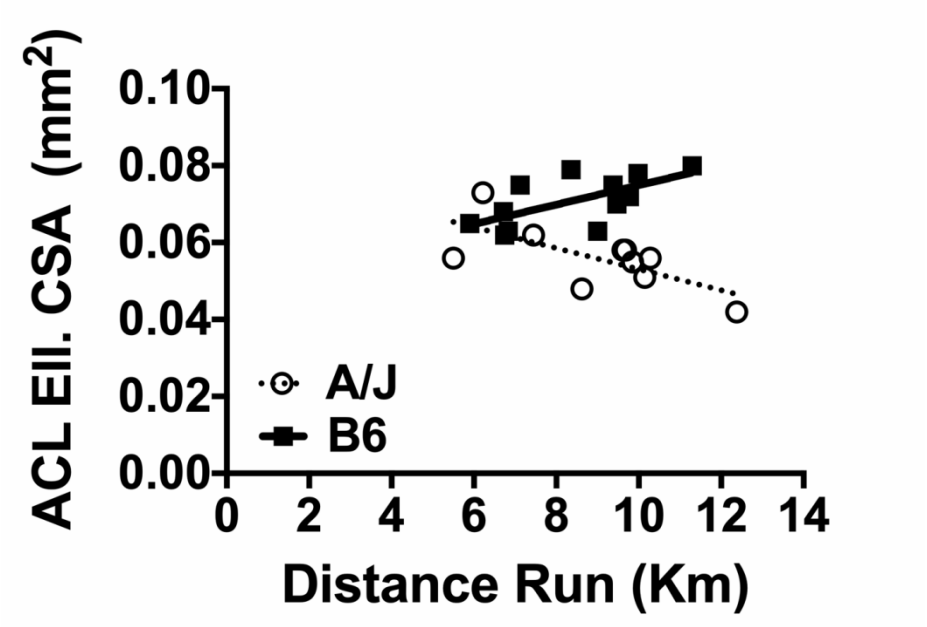

Figure 5. Calcified fibrocartilage depth across the tidemark (TM) for runners and controls of both inbred strains. A) A/J Fem.CF.De; B) B6 Fem.CF.De; C) A/J Tib.CF.De; and D) B6 Tib.CF.De. * denotes significance at $p < 0.05$.

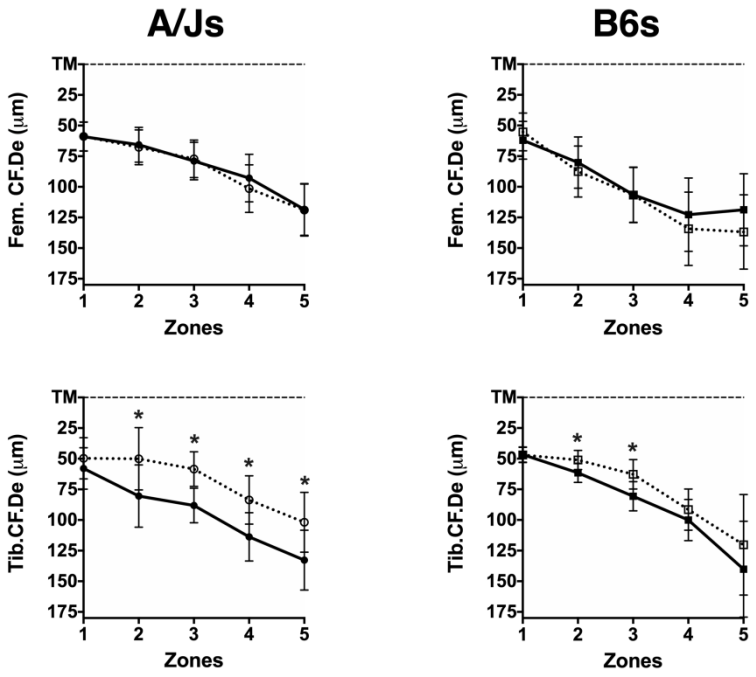

References

1. Viidik A. 1968. Elasticity and tensile strength of the anterior cruciate ligament in rabbits as influenced by training. Acta Physiol Scand 74:372-380.

2. Cabaud HE, Chatty A, Gildengorin V, Feltman RJ. 1980. Exercise effects on the strength of the rat anterior cuciate ligament. Am J Sports Med 8:79-86.

3. Grzelak P, Podgorski M, Stefanczyk L, et al. 2012. Hypertrophied cruciate ligament in high performance weightlifters observed in magnetic resonance imaging. Int Orthop 36:1715-1719.

4. Chandrashekar N, Slauterbeck J, Hashemi J. 2005. Sex-based differences in the anthropometric characteristics of the anterior cruciate ligament and its relation to intercondylar notch geometry. Am J Sports Med 33:1492-1498.

5. Brandon M, Haynes P, Bonamo J, et al. 2006. The association between posterior-inferior tibial slope and anterior cruciate ligament insufficiency. Arthosc 22:894-899.

6. Giffin J, Vogrin T, Zantop T, et al. 2004. Effects of increasing tibial slope on the biomechanics of the knee. Am J Sports Med 32:376-382.

7. Lipps D, Oh Y, Ashton-Miller J, Wojtys E. 2012. Morphologic characteristics help explain the gender difference in peak anterior cruciate ligament strain during a simulated pivot landing. Am J Sports Med 40:32-40.

8. Lipps D, Wojtys E, Ashton-Miller J. 2013. Anterior cruciate ligament fatigue failures in knees subjected to repeated simulated pivot landings. Am J Sports Med 41:1058-1066.

9. Chaudhari A, Zelman E, Flanigan D, et al. 2009. Anterior cruciate ligament-injured subjects have smaller anterior cruciate ligaments than matched controls: a magnetic resonance imaging study. Am J Sports Med 37:1282-1287.

10. Keays S, Keays R, Newcombe P. 2016. Femoral intercondylar notch width size: a comparison between sibliings with and without anterior cruciate ligament injuries. Knee Surg Sports Traumatol Arthrosc 24:672-679.

11. Simon R, Everhart J, Nagaraja H, Chaudhari A. 2010. A case-control study of anterior cruciate ligament volume, tibial plateau slopes and intercondylar notch dimensions in ACL-injured knees. J Biomech 43:1702-1707.

12. Beynnon B, Hall J, Sturnick D, et al. 2014. Increased slope of the lateral tibial plateau subchondral bone is associated with greater risk of noncontact ACL injury in females but not in males. Am J Sports Med 42:1039-1048.

13. Bojicic K, Beaulieu M, D.Y. IK, et al. 2017. Association between lateral posterior tibial slope, body mass index, and ACL injury risk. Orthop J Sports Med 5:7.

14. Tuca M, Hayter C, Potter H, et al. 2016. Anterior cruciate ligament and intercondylar notch growth plateaus prior to cessation of longitudinal growth: an MRI observational study. Knee Surg Sports Traumatol Arthrosc 24:780-787.

15. Price M, Tuca M, Cordasco F, Green DW. 2017. Nonmodifiable risk factors for anterior cruciate ligament injury. Curr Opin Pediatr 29:55-64.

16. Bass SL, Saxon L, Daly RM, et al. 2002. The effect of mechnical loading on the size and shape of bone in pre-, peri-, and postpubertal girls: a study in tennis players. J Bone Miner Res 17:2274-2280.

17. Macdonald H, Kontulainen S, MacKelvie-O'Brien K, et al. 2005. Maturity- and sex-related changes in tibial bone geometry, strength and bone-muscle strength indices during growth: a 20-month pQCT study. Bone 36:1003-1011.

18. Moro M, van der Meulen M, Kiralti BJ, et al. 1996. Body mass is the primary determinant of midfemoral bone acquisition during adolescent growth. Bone 19:519-526.

19. Kanehisa H, Ikegawa S, Tsunoda N, Fukunaga T. 1994. Cross-sectional areas of fat and muscle in limbs during growth and middle age. Int J Sports Med 15:420-425.

20. Rogol A, Roemmich J, Clark P. 2002. Growth at puberty. J Adolesc Health 31:192-200.

21. Ruff C. 2003. Growth in bone strength, body size, and muscle size in a juvenile longitudinal sample. Bone 33:317-329.

22. Dowling B, Dart A. 2005. Mechanical and functional properties of the equine superficial digital flexor tendon. Vet J 170:184-192.

23. O'Brien FJ, Hardiman DA, Hazenberg JG, et al. 2005. The behaviour of microcracks in compact bone. Eur J Morph 42:71-79.

24. Daly RM, Saxon L, Turner CH, et al. 2004. The relationship between muscle size and bone geometry during growth and in response to exercise. Bone 34:281– 287.

25. Kasashima Y, Smith R, Birch H, et al. 2002. Exercise-induced tendon hypertrophy: cross-sectional area changes during growth are influenced by exercise. Equine Exerc Physiol 34:264-268.

26. Kontulainen S, Sievanen H, Kannus P, et al. 2003. Effect of long-term impact-loading on mass, size, and estimated strength of humerus and radius of female racquet-sports players: a peripheral quantitative computed tomography study between young and lod starters and controls. J Bone Miner Res 18:352-359.

27. Vicente-Rodriguez G, Jimenez-Ramirez J, Ara I, et al. 2003. Enhanced bone mass and physical fitness in prepubescent footballers. Bone 33:853-859.

28. Vicente-Rodriguez G. 2005. How does exercise affect bone development and growth. Sports Med 36:561-569.

29. Carballo C, Hutchinson I, Album Z, et al. 2018. Biomechanics and microstructural analysis of the mouse knee and ligaments. J Knee Surg 31:520-527.

30. Wang V, Banack T, Tsai C, et al. 2006. Variability in tendon and knee joint mechanics among inbred mouse strains. J Orthop Res 24:1200-1207.

31. Beaulieu M, Carey G, Schlecht S, et al. 2015. Quantitative comparison of the microscopic anatomy of the human ACL femoral and tibial entheses. J Orthop Res 33:1811-1817.

32. Beaulieu M, Carey G, Schlecht SH, et al. 2016. On the heterogeniety of the femoral enthesis of the human ACL: microscopic anatomy and clinical implications. J Exper Orthop 3:14.

33. Schlecht S, Ramcharan MA, Yang Y, et al. 2018. Differential adaptive response of growing bones from two female inbred mouse strains to voluntary cage-wheel running. J Bone Miner Res Plus 2:143-153.

34. Black B, Croom J, Eisen E, et al. 1998. Differential effects of fat and sucrose on body composition in A/J and C57BL/6 mice. Metabol 47:1354-1359.

35. Gallou-Kabani C, Vige A, Gross M-S, et al. 2007. C57BL/6J and A/J mice fed a high-fat diet delineate components of metabolic syndrome. Obesity 15:1996-2005.

36. Price C, Herman BC, Lufkin T, et al. 2005. Genetic variation in bone growth patterns defines adult mouse bone fragility. J Bone Miner Res 20:1983-1991.

37. Schlecht SH, Smith LM, Ramcharan MA, et al. 2017. Canalization leads to similiar whole bone mechnical function at maturity in two inbred strains of mice. J Bone Miner Res 32:1002-1013.

38. Hagenauer M, Perryman J, Lee T, Carskadon M. 2009. Adolescent changes in the homeostatic and circadian regulation of sleep. Dev Neurosci 31:276-284.

39. Kercmar J, Tobet S, Majdic G. 2014. Social isolation during puberty affects female sexual behavior in mice. Front Behav Neurosc 8:337.

40. Dutta S, Sengupta P. 2016. Men and mice: relating their ages. Life Sci 152:244-248.

41. Fitch R, Montgomery R, Milton J, et al. 1995. The intercondylar fossa of the normal canine stifle an anatomic and radiographic study. Vet Surg 24:148-155.

42. Comerford E, Tarlton J, Avery N, et al. 2006. Distal femoral intercondylar notch dimensions and their relationship to composition and metabolism of the canine anterior cruciate ligament. Osteoarthr Cartilage 14:273-278.

43. Reif U, Probst C. 2003. Comparison of tibial plateau angles in normal and cranial cruciate deficient stifles of Labrador Retrievers. Vet Surg 32:385-389.

44. Evans EJ, Benjamin M, Pemberton DJ. 1990. Fibrocartilage in the attachment zones of the quadriceps tendon and patellar ligament of man. J Anat 171:155-162.

45. Morrison J. 1969. Function of the knee joint in various acivities. Biomed Eng 4:573-580.

46. Morrison J. 1970. The mechanics of the knee joint in relation to normal walking. J Biomech 3:51-61.

47. Chaudhari A, Andriacchi T. 2006. The mechanical consequences of dynamic frontal plane limb alignment for non-contact ACL injury. J Biomech 39:330-338.

48. Hewett TE, Myer G. 2011. The mechanistic connection between the trunk, knee, and anterior cruciate ligament injury. Exerc Sport Sci Rev 39:161-166.

49. Wojtys E, Beaulieu M, Ashton-Miller J. 2016. New perspectives on ACL injury: on the role of repetitive sub-maximal knee loading causing ACL fatigue failure. J Orthop Res 34:2059-2068.

50. Yamaguchi K, Cheung E, Mathew J, et al. 2017. ACL force and knee kinematics after posterior tibial slope-reducing osteotomy. Orthop J Sports Med 5:suppl6.

51. Benjamin M, Toumi H, Ralphs JR, et al. 2006. Where tendons and ligaments meet bone: attachment sites (‘entheses’) in relation to exercise and/or mechanical load. J Anat 208:471–490.

52. Girgis F, Marshall J, Monajem A. 1975. The cruciate ligaments of the knee joint. Anatomical, functional and experimental analysis. Clin Orthop Relat Res 106:216-231.

53. Sturnick D, Vacek P, DeSarno M, et al. 2015. Combined anatomic factors predicting risk of anterior cruciate ligament injury for males and females. Am J Sports Med 43:839-847.

54. Gornitzky A, Lott A, Yellin J, et al. 2017. Sport-specific yearly risk and incidence of anterior cruciate ligament tears in high school athletes: a systematic review and meta-analysis. Pediatr 140:109.

55. Weber A, Bach Jr. B, Bedi A. 2017. How do we eliminate risk factors for ACL injury? In: Musahl V, Karlsson J, Kuroda R, et al. editors. Rotatory Knee Instability. Switzerland: Springer; pp. 465-472.

56. Svensson M, Rosvall P, Boza-Serrano A, et al. 2016. Forced treadmill exercise can induce stress and increase neuronal damage in a mouse model of global cerebral ischemia. Neurobiol Stress 5:8-18.

57. De Bono J, Adlam D, Paterson D, Channon K. 2006. Novel quantitative phenotypes of exercise training in mouse models. Am J Physiol Regulat Inegrat Comp Physiol 290:R926-R934.

58. Tipton C, Schild R, Tomanek R. 1967. Influence of physcial activity on the strength of knee ligaments in rats. Am J Physiol 212:783-787.

59. Poliachik SL, Threet D, Srinivasan S, Gross TS. 2008. 32 wk old C3H/HeJ mice actively respond to mechanical loading. Bone 42:653-659.

60. Hall D, Poussin C, Velagapudi V, et al. 2010. Peroxisomal and microsomal lipid pathways associated with resistance to hepatic steatosis and reduced pro-inflammatory state. J Biol Chem 285:31011-31023.

61. Rubin CT, Lanyon LE. 1984. Dynamic strain similarity in vertebrates: an alternative to allometric limb bone scaling. J Theoret Biol 107:321-327.

Tables

Table 1. Frequently used abbreviations.

Femoral measures
ACL Ell.CSA: ACL elliptical cross-sectional area
Fem.Le: Maximum femur length
ANWI: Anterior femoral notch width index
CNWI: Central femoral notch width index
PNWI: Posterior femoral notch width index
NSI: Femoral notch shape index
Fem.Bicon.Wi: Femoral bicondylar width
Fem.TM.Le: Femoral enthesis tidemark length
Fem.CF.De: Femoral calcified fibrocartilage depth
Fem.CF.Ar: Femoral calcified fibrocartilage area
Tibial measures
Tib.Le: Maximum tibial length
Tib.Bicon.Wi: Tibial bicondylar width
PMTS: Posterior medial tibial plateau slope
PLTS: Posterior lateral tibial plateau slope
Tib.TM.Le: Tibial enthesis tidemark length

Tib.CF.Ar: Tibial calcified fibrocartilage area

Tib.CF.De: Tibial calcified fibrocartilage depth

Table 2. Mean and standard deviations of all key morphological traits quantified after adjusting for body weight. Percent differences are given for mean difference between control and exercise group of each strain. Bold denotes significance at p < 0.10.

		A/J			B6		
		Control	***Exercise***	***Diff***	***Control***	***Exercise***	***Diff***
Fem. Traits	Fem.Le (mm)	14.40 ±0.32	14.30 ±0.11	-0.69%	14.87 ±0.16	14.60 ±0.16	**-1.85%**
	Fem.Bicon.Wi (mm)	2.097 ±0.037	2.022 ±0.089	**-3.57%**	2.148 ±0.054	2.166 ±0.069	-0.82%
	ANWI (mm/mm)	0.154 ±0.023	0.139 ±0.018	-9.37%	0.200 ±0.020	0.188 ±0.031	-5.91%
	CNWI (mm/mm)	0.241 ±0.025	0.218 ±0.018	**-9.49%**	0.293 ±0.0144	0.290 ±0.021	-0.88%
	PNWI (mm/mm)	0.291 ±0.013	0.272 ±0.023	**-6.45%**	0.337 ±0.015	0.343 ±0.015	1.92%

	NSI (mm/mm)	0.665 ±0.069	0.530 ±0.068	**-19.06%**	0.696 ±0.042	0.665 ±0.041	**-5.89%**
Tib. Traits	Tib.Le (mm)	16.53 ±0.68	16.59 ±0.40	-0.35%	17.20 ±0.54	16.64 ±0.42	**-3.27%**
	Tib.Bicon.Wi (mm)	2.69 ±0.028	2.686 ±0.025	-0.27%	2.828 ±0.031	2.717 ±0.054	**-3.93%**
	PMTS (°)	25.23 ±1.44	24.08 ±1.00	**-4.57%**	26.05 ±1.32	28.70 ±1.34	**10.19%**
	PLTS (°)	24.32 ±1.50	22.34 ±2.35	**-8.15%**	32.46 ±2.64	31.33 ±1.50	-3.47%
ACL Traits	ACL Ell.CSA (mm^2)	0.060 ±0.008	0.056 ±0.008	-6.98%	0.062 ±0.007	0.071 ±0.007	**13.55%**
	Fem.TM.Le (μm)	174.2 ±13.7	184.0 ±28.6	5.59%	159.1 ±15.6	148.6 ±9.5	-6.61%
	Fem.CF.Ar (μm^2)	15147 ±1487	16387 ±1632	8.19%	15934 ±2390	14232 ±1032	**-10.68%**
	Fem.CF.De (μm)	84.82 ±3.80	83.00 ±12.47	-2.15%	103.71 ±13.41	99.08 ±9.28	-4.47%

	Tib.TM.Le (μm)	347.8 ±47.6	284.4 ±17.5	**-18.22%**	219.5 ±16.4	222.0 ±18.0	1.15%
	Tib.CF.Ar (μm^2)	28863 ±5746	22212 ±1217	**-23.04%**	19305 ±2356	17093 ±1363	**-11.46%**
	Tib.CF.De (μm)	60.73 ±5.45	75.55 ±8.87	**24.39%**	74.58 ±9.77	85.70 ±15.85	**14.90%**

Table 3. R^2 and p-values for each trait and their association with the daily distance run by exercise mice of each strain. Bold denotes significance at p < 0.05.

	A/J		**B6**	
Trait	***R^2***	***p***	***R^2***	***p***
ACL Ell.CSA (μm^2)	**0.46**	**0.03**	**0.41**	**0.02**
Fem.Bicon.Wi (mm)	0.04	0.52	0.02	0.88
ANWI (mm/mm)	0.16	0.22	<0.01	0.82
CNWI (mm/mm)	<0.01	0.82	<0.01	0.96
PNWI (mm/mm)	0.19	0.17	0.02	0.65
NSI (mm/mm)	0.15	0.23	0.13	0.27
Fem.TM.Le (μm)	0.26	0.20	**0.59**	**0.02**

Fem.CF.Ar (μm^2)	<0.01	0.93	0.12	0.81
Fem.CF.De (μm)	<0.01	0.88	0.08	0.53
Tib.Bicon.Wi (mm)	0.16	0.18	0.08	0. 66
Tib.TM.Le (μm)	0.04	0.65	0.01	0.71
Tib.CF.Ar (μm^2)	0.11	0.43	0.13	0.25
Tib.CF.De (μm)	<0.01	0.97	0.01	0.69
PMTS (°)	0.05	0.49	0.05	0.49
PLTS (°)	0.08	0.37	0.13	0.27